Origin of the lattice sites occupied by implanted Co in Si

2014 Semicond. Sci. Technol. 29 125006

(http://iopscience.iop.org/0268-1242/29/12/125006)

IOP Publishing Semiconductor Science and Technology
Semicond. Sci. Technol. **29** (2014) 125006 (5pp) doi:10.1088/0268-1242/29/12/125006

Origin of the lattice sites occupied by implanted Co in Si

D J Silva[1], U Wahl[2], J G Correia[2], L M C Pereira[3], L M Amorim[3], M R da Silva[4] and J P Araújo[1]

[1] IFIMUP and IN-Institute of Nanoscience and Nanotechnology, Departamento de Física e Astronomia da Faculdade de Ciências da Universidade do Porto, 4169–007 Porto, Portugal
[2] Centro de Ciências e Tecnologias Nucleares, Instituto Superior Técnico, Universidade de Lisboa, 2686–953 Sacavém, Portugal
[3] Instituut voor Kern- en Stralingsfysica, KU Leuven, B-3001 Leuven, Belgium
[4] Centro de Física Nuclear da Universidade de Lisboa, 1649–003 Lisboa, Portugal

E-mail: jearaujo@fc.up.pt

Received 5 July 2014, revised 15 September 2014
Accepted for publication 26 September 2014
Published 13 November 2014

Abstract

We have investigated the lattice location of implanted ^{61}Co in silicon. By means of emission channeling, three different lattice sites have been identified: ideal substitutional sites, displaced bond-centered sites and displaced tetrahedral interstitial sites. To assess the origin of the observed lattice sites we have compared our results to emission channeling studies on ^{59}Fe and ^{65}Ni and to Mössbauer spectroscopy experiments on ^{57}Co, present in literature. The possible interpretation of several ^{57}Co Mössbauer lines is discussed in the light of our new results on the ^{61}Co lattice location. The conclusions are relevant for the microscopic understanding of some gettering techniques.

Keywords: emission channeling, transition metals, silicon, cobalt

(Some figures may appear in colour only in the online journal)

1. Introduction

Together with other transition metals (TMs), Co introduces deep levels in the silicon bandgap. These deep levels depend on the complexes that Co forms [1], and are unwanted in most applications, e.g. causing efficiency degradation of solar cells. To avoid such harmful effects, gettering procedures, relying on moving the unwanted impurity away from the active area of devices, have been used, e.g., by introducing gettering centers through irradiation or by diffusing phosphorus [2]. Although a quantitative description of the macroscopic behavior of gettering procedures is now quite well established, the involved microscopic complexes are far from being understood and subject of ongoing discussions. Studies of the lattice location of the ion implanted radioactive 3d TM probes ^{67}Cu [3], ^{59}Fe [5, 6] and ^{65}Ni [7] with the emission Channeling (EC) technique have been previously exploring such complexes, and here we provide results on ^{61}Co. We note that the various types of lattice sites identified are also likely to be of relevance if the TMs are introduced by other processes than implantation, although quite likely with different abundancies. A certain shortcoming of the EC technique is its lack of sensitivity to the immediate local environment of the probe atoms, which complicates the identification of the complexes responsible for the observed lattice sites. In that respect, ^{57}Co → ^{57}Fe Mössbauer spectroscopy (MS) is a complementary technique, since it gives information on the charge distribution in the local environment of the probe atom via the hyperfine interaction. The comparison of ^{61}Co lattice location (via EC of emitted electrons) and ^{57}Co hyperfine interaction (via MS of emitted gamma particles), hence offers the opportunity to provide a more detailed understanding. We will therefore also critically assess the interpretation of MS results for implanted ^{57}Co in Si in the literature [8–10].

In this work, we have investigated experimentally the lattice location of ^{61}Co ($t_{1/2}$ = 1.65 h) in monocrystalline silicon by means of EC with short-lived isotopes (EC-SLI). ^{61}Co was produced, introduced in the silicon sample and measured at CERN's ISOLDE facility. In EC-SLI

experiments, the preferred lattice sites can be derived from the strong dependence of the channeling effects of the emitted β^- particles on the sites occupied by the short lived probe atoms [7, 11–14]. We compare our results to EC studies on ^{59}Fe [5, 6] and ^{65}Ni [7], and to MS experiments from [8–10].

2. Experiment and method of analysis

The sample used was *n*-type Si with a resistivity of 7.3–12 Ωcm and a <111> surface. In order to dope the silicon sample with ^{61}Co, the precursor isotope ^{61}Mn was implanted with an energy of 50 keV under a tilt angle of 17°. ^{61}Mn was converted into ^{61}Co as a result of the decay chain ^{61}Mn ($t_{1/2}$ = 0.61 s) → ^{61}Fe (5.98 min) → ^{61}Co (1.65 h). Since the recoil energy of the ^{61}Fe decay (103 eV [13]) is well above the average threshold displacement energy in silicon (36 eV [15]), the resulting ^{61}Co was re-implanted, avoiding therefore the influence of the sites occupied by ^{61}Fe. The annealing treatment and emission channeling measurements took place only ~30 min after each implantation stop, to be sure that ^{61}Fe was not present in significant quantities. Hence, if despite the 103 eV recoil any of the ^{61}Co probes should have survived on the same lattice sites as ^{61}Fe, the interaction with their surroundings during thermal treatment happened when the chemical nature of the probe was Co and should hence characterize the behaviour of this element. Due to the short half-life of ^{61}Co and its continuous decay into ^{65}Ni, the amount of ^{61}Co left in the sample at the end of each measurement is negligible. However, at the beginning of the last measurement of the experiment more than ten times as much stable ^{61}Ni than radioactive ^{61}Co has accumulated. Therefore, while each measured two-dimensional pattern was not influenced by the previous observed lattice sites of ^{61}Co, the accumulated ^{61}Ni content, though very small, might have played a role to some extent, e.g. in interacting with ^{61}Co. Also, in the course of the experiment, radiation damage will increase in the sample according to the detailed implantation and annealing history.

^{61}Mn was implanted in 9 steps of ~1.5×10^{12} cm^{-2}. While after the first implantation step the sample was measured as-implanted at room temperature (RT), each successive implantation step was followed by annealing *in situ* for 10 min at a given temperature, applying 150 °C, 300 °C, 400 °C, 475 °C, 550 °C, 650 °C, 750 °C and 850 °C. The two-dimensional EC patterns were measured at room temperature after each anneal in the vicinity of <110>, <211>, <100> and <111>, by using a position and energy sensitive detector. The electrons that reach the detector after being backscattered inside the sample or from the wall of the vacuum chamber were considered by subtracting an isotropic background, obtained with the Monte Carlo electron scattering simulation code GEANT4 [16]. The whole experiment was performed inside an on-line chamber [17].

The depth profile of the implanted ^{61}Mn was obtained using the SRIM code [18]. It can be approximated by a Gaussian centered at 463 Å from the surface with a straggling of 180 Å and a peak of 3.8×10^{17} cm^{-3} (for each of the implantation steps). Each implanted ^{61}Mn ion produces approximately 700 vacancies. The depth profile of produced vacancies is centered approximately half way from the surface to the peak concentration of ^{61}Mn (so-called '$R_p/2$' region). The vacancy peak concentration is ~3×10^{20} cm^{-3}, also for each implantation step.

In order to obtain the occupied lattice sites of ^{61}Co, the two-dimensional experimental patterns were fitted using calculated β emission yields, obtained with the *manybeam* formalism for electron channeling in single crystals [19]. The emission probability of the substitutional (S), hexagonal (H), tetrahedral (T), bond-centered (BC), anti-bonding (AB), split <100> (SP), <110> displaced substitutional (DS), <110> displaced tetrahedral (DT), ytterbium (Y) and carbon (C) sites, as well as <111>, <100> and <110> displacements between these positions, were included in the fitted patterns. The detailed location of these sites within the Si lattice has been described in figure 1 of [7]. When fitting with only one fraction three types of sites resulted in the best fits, depending on the annealing temperature. For low annealing temperatures the best fits were obtained considering sites displaced from BC towards ideal S sites (near-BC sites), while for high annealing temperatures the best fits resulted from ideal S sites. At intermediate annealing temperatures, sites displaced from T towards AB sites (near-T sites) resulted in the lowest χ^2 of fit. A second fitting procedure was therefore performed by considering these three lattice sites at the same time.

3. Results and discussion

Figure 1 shows the two-dimensional experimental and best fit EC patterns in the vicinity of <110> for all the studied annealing temperatures, and the corresponding dependence of the site fractions on the annealing temperature. Figure 2 also shows the emission channeling patterns for the remaining three orientations <100>, <211> and <111>, after the 550 °C anneal. While near-BC and near-T sites were present in a continuous range of annealing temperatures, the ideal S fraction was considerably reduced at intermediate annealing temperatures. It seems thus possible that the complex structure with Co sitting on ideal substitutional sites may be different for low and high annealing temperatures.

At this point it is worthwhile mentioning that the overall trend of the ^{61}Co lattice location as a function of annealing temperature shows considerable similarities to our previous results on ^{59}Fe [5, 6] and ^{65}Ni [7] in Si samples of similar doping type, i.e. neither highly *n*- nor highly *p*-type Si. For all three elements at low annealing temperatures near-BC sites were quite prominent, followed by an intermediate annealing temperature regime, starting around 400–500 °C, where interstitial sites near the T position were dominating. However, while for ^{61}Co and ^{59}Fe at the highest annealing temperatures ideal substitutional sites were increasingly contributing, in the case of ^{65}Ni the emission channeling effects already nearly disappeared after annealing at 600 °C.

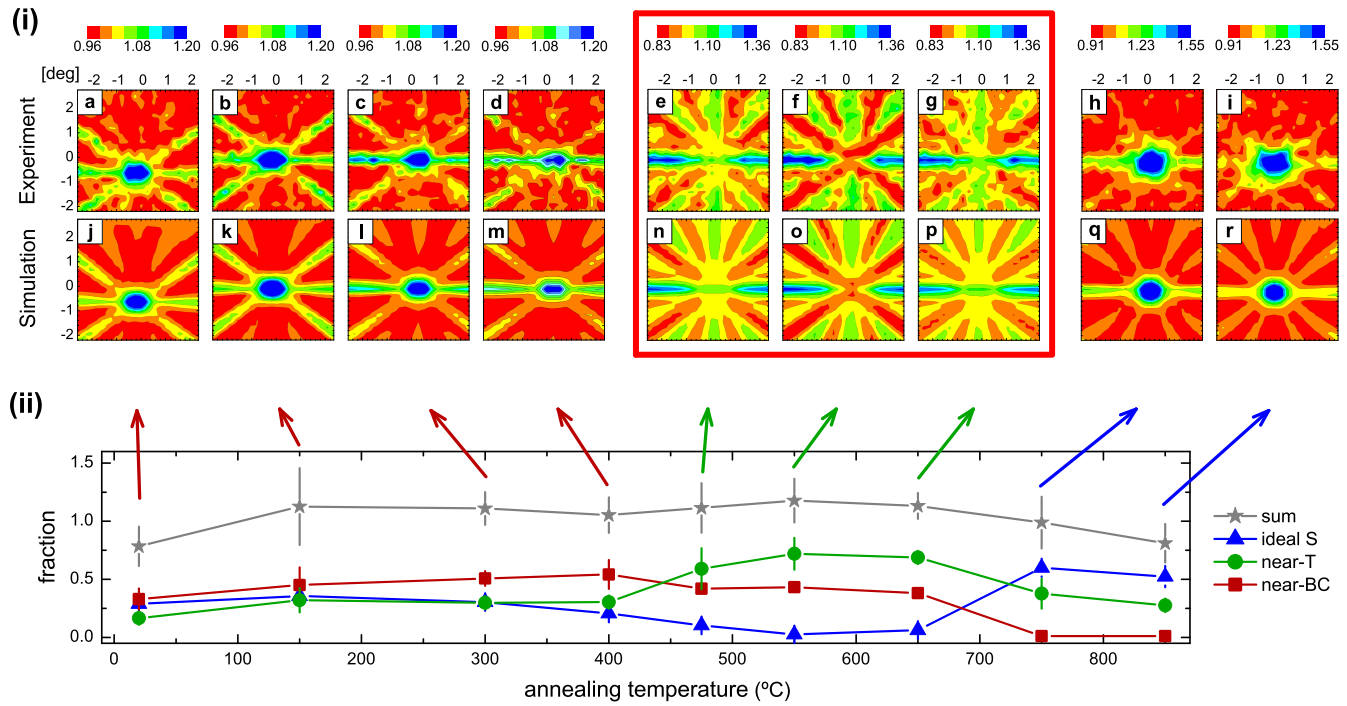

Figure 1. (**i**) Comparison of the two-dimensional experimental and best fit of simulated emission channeling patterns from ^{61}Co in *n*-type Si in the vicinity of <110>, after room temperature implantation (**a**,**j**) and after annealing at 150 °C (**b**,**k**), 300 °C (**c**,**l**), 400 °C (**d**,**m**), 475 °C (**e**, **n**), 550 °C (**f**,**o**), 650 °C (**g**,**p**), 750 °C (**h**,**q**) and 850 °C (**i**,**r**). (**ii**) Fractions of the three observed lattice sites ideal S, near-T sites and near-BC sites as a function of annealing temperature.

The fact that near-BC sites and near-T sites were found in all three cases and with a relatively similar dependence on annealing temperature, suggests that the underlying defects are formed via a mechanism that may be common to all three of these transition metals. Our interpretation in the case of ^{59}Fe and ^{65}Ni had been that the near-BC sites are associated with transition metals that are located in the center of a divacancy or within more extended vacancy-type complexes, such as fourfold hexavacancy clusters [6, 7, 20]. We also suggest this interpretation here for ^{61}Co. The nature of the near-T sites was far less clear. Regarding the near-T sites, we had tentatively suggested that they may result from ^{59}Fe and ^{65}Ni on metastable positions next to a vacancy or divacancy. While in the case of ^{59}Fe in low-doped Si the prominent occupation of near-T sites was apparently accompanied by Fe diffusing into the damage-rich '$R_p/2$' region, such diffusion was not obvious for ^{65}Ni or ^{61}Co.

To compare the observed emission channeling sites in this work with the Mössbauer lines from [8–10, 21] it is imperative to discuss first the differences and similarities of the experimental conditions. The probe investigated by MS was ^{57}Co ($t_{1/2}$ = 270 d) which decays by capturing an electron from the inner shell and by gamma emission into the well-known ^{57m}Fe ($t_{1/2}$ = 98 ns) state. The Mössbauer effect measurement takes place subsequently when the ^{57m}Fe state de-excites to the ground state, hence on a Fe impurity. While the ^{57}Co electron capture decay transfers only a small recoil energy of 4.6 eV to its ^{57*}Fe daughter nucleus, which is probably not enough to displace it from its lattice site, the transfer of kinetic energy might certainly result in structural

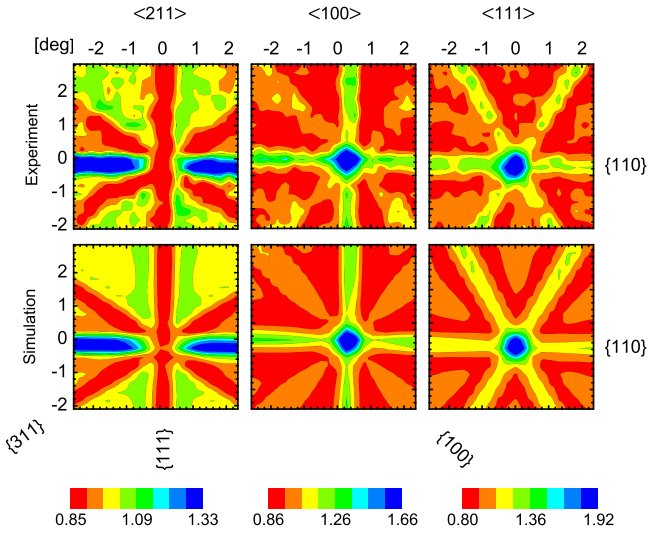

Figure 2. Two-dimensional experimental and calculated emission channeling patterns from ^{61}Co in *n*-type Si, in the vicinity of <211>, <100>, and <111>, following annealing at 550 °C.

configurations of the Fe defect that are different from the Co precursor. Also, since initially its innermost electron is missing, the electronic shell of ^{57}Fe subsequently undergoes a complete restructuring by means of x-ray and Auger electron emission, at the end of which the Fe impurity may be left in a charge state that does not correspond to thermal equilibrium for an Fe impurity either. However, the 98 ns half-life of ^{57m}Fe is much smaller than the time taken by the fast interstitial diffuser Fe to make one diffusion step at room

temperature (~300 ms). Summarizing, the Mössbauer effect from ^{57}Co measures on a Fe impurity whose structural properties, however, are probably still influenced by those of the ^{57}Co precursor. On the other hand, in β^- emission channeling experiments, the emitted β^- particles characterize the lattice location of the ^{61}Co impurity in thermal equilibrium. Another important parameter for comparing both experiments is the fluence. For the case of MS the fluence ranged from 2.5×10^{12} to 1×10^{13} cm^{-2} and was applied in a single implantation, corresponding to peak concentrations between 1×10^{17} and 1×10^{18} cm^{-3}. We note, however, that the presence of the Mössbauer lines that will be compared with the EC lattice sites inferred from this work appeared for the lower fluence case.

For low annealing temperatures (⩽400 °C) MS only observes the singlet line assigned to ideal substitutional sites and the 'amorphous' doublet [8, 9, 21]. While one would expect that the 'amorphous' doublet in MS directly corresponds to the random sites in EC, the related fractions do not match: in the RT as-implanted state and in the 10^{11}–10^{12} cm^{-2} fluence range, the 'amorphous' doublet accounts for ~80% of the spectral intensity (with the remaining ~20% being substitutional singlet) [9], while the random fraction in our EC experiment, under similar conditions, is only ~20% (with ~27% identified on ideal S, ~30% on near-BC and ~15% on near-T). On the other hand, one would expect that MS probes on any type of near-BC site are subject to an electrical field gradient since their environment is not of cubic symmetry. It hence seems as if the 'amorphous' doublet is actually a combination of several sites that are characterized by similar electric field gradients, most likely including the random as well as the near-BC sites identified by EC.

For annealing temperatures of 475–650 °C [figure 1 (**ii**)], the dominating ^{61}Co fraction in emission channeling are the near-T sites, with maximum fractions around 70%. They become prominent in a similar temperature range where a second Mössbauer quadrupole doublet line appears (400–450 °C) with maximum fractions around 40% [8, 9, 21]. The range of annealing temperatures up to which the near-T fraction and this second quadrupole doublet prevail is not exactly the same, ~475–500 °C in the MS experiments and 475–650 °C in EC. However, this can possibly be explained by the fact that the annealing treatments of [8] lasted 1 h (under Ar atmosphere), which could have broken up the complexes associated with this Mössbauer line already at 500 °C, while in the EC experiments 10 min annealing was used. Also, the much longer measuring times in MS may have played a role and caused the premature annealing of the doublet line. It should also be noted that the resistivities of the samples in the investigation of [8] were both *n*- and *p*-type Si FZ of 0.06–0.13 Ωcm, while in this work we studied only *n*-type Si CZ with 7.3–12Ωcm, i.e. a sample that is more intrinsic than the two types of Si samples used in the MS studies. As mentioned in [8, 9] the quadrupole doublet lines were visible both in *n*- and *p*-type Si, although being much more prominent in *n*-type material. Hence, there is good reason to expect them, although less prominent, in the type of sample used in our study. Remarkably, this second Mössbauer quadrupole doublet was suggested to be due to the formation of dimers of two Co atoms [8, 9, 21]. However, as we will outline in the following, this interpretation poses quite some inconsistencies and we hence consider it doubtful. First of all, the MS quadrupole doublet was identified as Co dimers despite the fact that its relative intensity compared to the total spectrum area was found to be inversely proportional to the Co concentration: it dominated the Mössbauer spectrum at 2.5×10^{12} cm^{-2} but was barely visible at fluences above 10^{14} cm^{-2}. While one would expect that a defect containing two Co atoms would have a higher probability of being formed when the Co concentration is increased, it was proposed in [8, 9] that already in the low 10^{12} cm^{-2} range one is in a regime where the formation of higher order Co clusters dominates over the formation of dimers above 500 °C. Consequently, irrespective of fluence, any ^{57}Co MS signal in Si observed after annealing above 500 °C was attributed to even higher-order Co clusters, Co silicides, or segregation of Co to the surface. We note that it is easy to estimate that, if Co dimers would be formed in, e.g., 2.5×10^{12} cm^{-2} implanted samples, there should be a mechanism that very efficiently pairs two Co atoms even if their initial separation would be more than 200 Å and despite a considerable number of implantation-related defects that survive 500 °C annealing and may trap them. Moreover, in the MS experiments there was only one quadrupole doublet found. If this would result from Co dimers, it clearly means that the two Co atoms occupy equivalent sites since otherwise the defect would give rise to two different quadrupole doublets, as was also pointed out in [21]. The only structural model proposed so far for a Co-dimer with two Co atoms on equivalent sites is a pair of substitutional Co atoms that are in a complex with a Si interstitial [21], requiring actually three constituents. This model, however, is clearly not backed by the emission channeling results, which find an increase in the near-T fraction at 475 °C, suggesting that if Co dimers were to form at this temperature they would involve at least one interstitial Co atom, or consist of two interstitial Co atoms that are both displaced from the ideal T site. It is also not backed by [22], which suggests the most stable configuration of Co dimers being a substitutional Co atom paired with a Co interstitial. Summarizing, while the formation of Co dimers cannot be ruled out with certainty, there exists currently no microscopic model for such dimers that could consistently explain both the Mössbauer and emission channeling results.

Finally, annealing above 750 °C caused the majority of ^{61}Co to occupy ideal substitutional sites. In ^{57}Co MS single lines and doublets observed in Si at such high annealing temperatures were generally associated with Co silicides [9]. In that respect, one may consider the question whether the observation of S sites at high annealing temperatures is due to the formation of epitaxial silicide precipitates [23]. Since the characteristic of substitutional Si sites, as observed by our emission channeling experiments, is that the ^{61}Co probe atoms are perfectly aligned with each crystallographic direction of the Si matrix, this puts considerable constraints on the

possible structure of the silicide precipitate. For instance, $CoSi_2$ exhibits the calcium fluoride structure which can be obtained from the diamond structure of Si by replacing one fcc sublattice of Si with Co atoms and, in addition to the second fcc lattice of Si, filling also all interstitital T sites with additional Si atoms. ^{61}Co probes in such a structure would in fact produce S-like emission channeling patterns but only if the precipitate expands within the surrounding Si matrix so that the 1.2% lattice mismatch of relaxed $CoSi_2$ with Si is completely removed by strain. In that respect it should be pointed out that the Mössbauer single lines identified as substitutional ^{57}Co [24] and ^{57}Co in $CoSi_2$ [9] have very similar isomer shift, so that they are in any case difficult to distinguish. We should also note the fact that due to the short half-life of ^{61}Co and its continuous decay into ^{61}Ni, the actual amount of ^{61}Co in our sample at any given time was very small, usually less than 10^{12} cm^{-2}, while at the end of the experiment more than ten times as much stable ^{61}Ni has accumulated. Summarizing, our interpretation is that in low-fluence implanted samples, even after annealing at 850 °C the substitutional Co fraction does not represent silicide precipitates but still single Co atoms, or at most aggregates of a small number of Co atoms that still allow all of them to occupy substitutional Si sites.

4. Conclusion

The comparison of the identified lattice sites (ideal S, near-BC and near-T) with the Mössbauer lines reported in literature allowed us to obtain a more differentiated picture of the complexes formed by implanted Co in Si. In particular, we propose that the Co visible on near-BC sites in emission channeling experiments, where the related structure has recently been suggested to be involved in P-diffusion gettering of Fe and Ni [6, 7], forms a part of the 'amorphous' doublet line seen in ^{57}Co Mössbauer spectroscopy. This point of view fits well with our previous interpretations of similar near-BC sites for ^{59}Fe and ^{65}Ni, which we attributed to the transition metals being located inside double and multiple vacancies. The local atomic structure around the transition metal would be characterized by somewhat varying bond lengths and angles which may result in Mössbauer parameters quite similar to an amorphous matrix. In addition, we showed that ^{61}Co atoms occupy sites displaced from tetrahedral interstitial towards anti-bonding sites in about the same annealing temperature range where ^{57}Co MS observes a distinctive quadrupole doublet that was previously suggested to result from the formation of Co dimers. We have presented arguments why we consider the interpretation as Co dimers doubtful. Finally, the ideal S sites observed by emission channeling at the highest annealing temperatures represent most likely still single Co atoms or clusters of few substitutional Co atoms involved in the first stages of precipitation. If ^{61}Co should be found within silicide precipitates, our data are only compatible with transition metal precipitates where the ^{61}Co atoms would be perfectly aligned with the surrounding Si matrix.

Acknowledgments

This work was supported by FCT-Portugal, project CERN-FP-123585-2011 and by the European Union FP7-through ENSAR, contract 262010. Project Norte-070124-FEDER-000070 is acknowledged. D J Silva is grateful for FCT Grant SFRH/BD/69435/2010. The authors further acknowledge the ISOLDE collaboration for supportive access to beam time.

References

[1] Weber E R 1983 *Appl. Phys. A: Solids Surf.* **30** 1
[2] Myers S M, Seibt M and Schröter W 2000 *J. Appl. Phys.* **88** 3795
[3] Wahl U, Vantomme A, Langouche G and Correia J G 2000 *Phys. Rev. Lett.* **84** 1495
[4] Wahl U, Vantomme A, Langouche G, Araújo J P, Peralta L and Correia J G 2000 *Appl. Phys. Lett.* **77** 2142
[5] Wahl U, Correia J G, Rita E, Araújo J P and Soares J C 2005 *Phys. Rev.* B **72** 014115
[6] Silva D J, Wahl U, Correia J G and Araújo J P 2013 *J. Appl. Phys.* **114** 103503
[7] Silva D J, Wahl U, Correia J G, Pereira L M C, Amorim L M, Bosne E, da Silva M R and Araújo J P 2014 *J. Appl. Phys.* **115** 023504
[8] Langouche G, Potter M D and Schroyen D 1984 *Phys. Rev. Lett.* **53** 1364
[9] Langouche G, Potter M D, Dézsi I, Wu M F and Vantomme A 1989 *Nucl. Instrum. Methods Phys. Res.* B **37** 438
[10] Gilles D, Schröter W and Bergholz W 1990 *Phys. Rev.* B **41** 5770
[11] Wahl U, Vantomme A, Langouche G, Araújo J P, Peralta L and Correia J G 2000 *Appl. Phys. Lett.* **77** 2142
[12] Pereira L M, Wahl U, Decoster S, Correia J G, Silva M R D, Vantomme A and Araújo J P 2011 *Appl. Phys. Lett.* **98** 201905
[13] Pereira L M C, Wahl U, Decoster S, Correia J G, Amorim L M, Silva M R D, Araújo J P and Vantomme A 2011 *Phys. Rev.* B **84** 125204
[14] Pereira L M C, Wahl U, Correia J G, Amorim L M, Silva D J, Bosne E, Decoster S, da Silva M R, Temst K and Vantomme A 2013 *Appl. Phys. Lett.* **103** 091905
[15] Holmström E, Kuronen A and Nordlund K 2008 *Phys. Rev.* B **78** 045202
[16] Agostinelli S *et al* 2003 *Nucl. Instrum. Methods Phys. Res.* A **506** 250
[17] da Silva M R, Wahl U, Correia J G, Amorim L M and Pereira L M C 2013 *Rev. Sci. Instrum.* **84** 073506
[18] Ziegler J F, Ziegler M D and Biersack J P 2010 *Nucl. Instrum. Methods Phys. Res.* B **268** 1818
[19] Wahl U, Correia J G, Cardoso S, Marques J G, Vantomme A and Langouche G 1998 *Nucl. Instrum. Methods Phys. Res.* B **136** 744
[20] Makhov D V and Lewis L J 2004 *Phys. Rev. Lett.* **92** 255504
[21] Bavel A M V, Langouche G and Overhof H 1998 *Semicond. Sci. Technol.* **13** 108
[22] Zhang Z Z, Partoens B, Chang K and Peeters F M 2008 *Phys. Rev.* B **77** 155201
[23] Istratov A A and Weber E R 1998 *Appl. Phys.* A **66** 123
[24] Langouche G and Potter M D 1987 *Nucl. Instrum. Methods Phys. Res.* B **19** 322